



# An innovative approach in osteoporosis opportunistic screening by the dental practitioner: the use of cervical vertebrae and cone beam computed tomography with its viewer program

Imad Barnkggei, BDS, MSc,<sup>a,1</sup> Easter Joury, BDS, DOrth, MSc (Lond), PhD (Lond), MFDS RCPS (Glasg),<sup>b,c,1</sup> and Ali Jawad, MB, ChB MSc (Lond), FRCP<sup>d,e</sup>

**Objectives.** To investigate the use of cone beam computed tomography (CBCT) for predicting osteoporosis based on the cervical vertebrae CBCT-derived radiographic density (RD) using the CBCT-viewer program.

**Study Design.** CBCT scans (WhiteFox, de Gotzen S.r.l device, distributed by Satelec-Acteon Group, Italy) and dual-energy X-ray absorptiometry examinations of 38 women who participated in an earlier investigation were examined. A coronal slice, subjectively determined from the cervical vertebrae, was selected and the RD as gray values for the first and second vertebrae, and the dens was calculated by using CBCT-viewer software (WhiteFox imaging).

**Results.** The CBCT-derived RD values of the dens and the left part of the first cervical vertebra showed the strongest correlation coefficients ( $r = 0.7, 0.6; P < .001$ ) and the highest sensitivity (76.9%, 70%), specificity (92%, 92.9%), and accuracy (90.8%, 86.4%) in predicting osteoporosis in the lumbar vertebrae and the femoral neck, respectively.

**Conclusions.** CBCT-derived RD of cervical vertebrae can predict osteoporosis status using a CBCT-viewer program. This finding should be confirmed on other CBCT devices. (Oral Surg Oral Med Oral Pathol Oral Radiol 2015;120:651-659)

Osteoporosis is a major public health problem. It is a skeletal disease characterized by low bone mass, deterioration of the bone structure, and an increased risk of fracture.<sup>1</sup> Osteoporotic fractures may affect any area of the skeleton except the face. The most common sites are the hip, vertebrae, proximal humerus, and distal forearm.<sup>2-4</sup> Osteoporotic fractures are associated with significant morbidity and increased mortality, with 10% to 20% of women with hip fractures dying within the first year.<sup>5</sup> Two-thirds of vertebral fractures are painless. Mortality increases by 15% in patients with painful vertebral fractures.<sup>6</sup> Those who survive suffer from increasing disability with poor quality of life.<sup>5</sup> The financial burden of osteoporosis is substantial. It has been estimated that the annual medical costs of

management of acute fractures and rehabilitation range between US\$ 17 to 20 billion.<sup>7</sup> In addition, there are indirect monetary and nonmonetary costs (e.g., care time) that add to the financial and societal burden of this disease.<sup>7</sup> Early diagnosis is essential. However, the silent nature of osteoporosis delays diagnosis.<sup>8</sup> Health care professionals should collaborate to create an opportunity for early detection, timely diagnosis, and appropriate treatment. In dentistry, early detection is important because patients with osteoporosis may suffer from higher failure rates of dental implants.<sup>9</sup>

Dentists are commonly consulted by a large segment of the population. Dental radiographs are used for diagnosis of conditions affecting teeth and jaws. These radiographs may offer an opportunity to detect osteoporosis and have been suggested as a screening tool for the disease.<sup>10-12</sup>

Bone quality refers to the combination of all characteristics that influence its resistance to fracture.<sup>13</sup> Bone quality is best assessed if more of its characteristics are quantified. The degree of mineralization and trabecular microstructure are the strongest predictors of bone strength.<sup>14</sup>

This study was part of OSTEOSYR project, a fully funded MSc and PhD project by the Faculty of Dentistry in Damascus University, with the first author as the principle investigator.

<sup>1</sup>These authors contributed equally to this work.

<sup>a</sup>Oral Medicine Department, Faculty of Dentistry, Damascus University, Damascus, Syria.

<sup>b</sup>Assistant Professor of Dental Public Health and Oral Epidemiology, Oral Medicine Department, Faculty of Dentistry, Damascus University, Damascus, Syria.

<sup>c</sup>Centre for Oral Growth and Development, Barts and The London School of Medicine and Dentistry, Queen Mary University of London, London, United Kingdom.

<sup>d</sup>William Harvey Research Institute, Queen Mary University of London, London, United Kingdom.

<sup>e</sup>Royal London Hospital, London, United Kingdom.

Received for publication Feb 4, 2015; returned for revision Aug 6, 2015; accepted for publication Aug 12, 2015.

© 2015 Elsevier Inc. All rights reserved.

2212-4403/\$ - see front matter

<http://dx.doi.org/10.1016/j.oooo.2015.08.008>

## Statement of Clinical Relevance

When a cone beam computed tomography (CBCT) scan is available, dentists can use it as a screening tool for osteoporosis, which is a major public health problem among menopausal and postmenopausal women, without the need for expensive or complicated software or special training.

Cone beam computed tomography (CBCT) has been used widely since its introduction in dentistry in 1998.<sup>15,16</sup> The CBCT technique has many advantages. It offers 2- and 3-dimensional images for the radiographed area at a relatively low cost compared with multidetector computed tomography (MDCT). However, the radiation dose of CBCT scans differs greatly, depending on the exposure parameters (the field of views [FOV],<sup>17</sup> in particular). The radiation dose of large (maxillofacial) FOVs may be 8.4 to 19.4 and 1.4 to 13.1 times greater than that of small (partial jaw) and medium (dentoalveolar or single jaw) FOVs, respectively.<sup>18</sup> However, even small FOV scans can produce effective doses much greater than that in conventional dental radiography, depending on the parameters of the scanner. In addition, the radiation dose of CBCT is higher than that of conventional dental radiographs.<sup>19</sup> CBCT provides information on assessment of bone quality.<sup>17</sup> One of the basic prescription rules for radiation is that CBCT should only be used when conventional radiography cannot provide an answer to the clinical question.<sup>20</sup>

Manufacturers of CBCT devices offer a viewer software to study the images. This software has the necessary tools for basic and simple analyses, such as multiplanar reconstruction, dimensional measurements, and radiographic density (RD) measurements.

Few studies have used CBCT to evaluate the relationship between osteoporosis and jawbone CBCT-derived RD.<sup>21</sup> However, additional programs, special phantoms, or both have been used to analyze CBCT images. These complicated procedures would hinder the use of such a method as an opportunistic screening tool for osteoporosis. They also add to the cost.

We decided to test whether CBCT images can predict osteoporosis in menopausal and postmenopausal women by using the associated CBCT viewer program. This program is used by dentists because it is user-friendly and requires minimal training. We are unaware of any study that has evaluated the use of CBCT in predicting osteoporosis from the cervical vertebrae CBCT-derived RD. The aim of the present study was to evaluate the ability of CBCT images to predict osteoporosis from the cervical vertebrae CBCT-derived RD values in menopausal and postmenopausal women using the associated CBCT viewer program.

## METHODS AND MATERIALS

### Study design

The present study adopted an observational cross-sectional design. The sample sizes of 38 menopausal and postmenopausal women were estimated to detect a correlation coefficient of 0.4 and greater (medium and strong) between the cervical vertebrae CBCT-derived

RD values and lumbar vertebrae and femoral neck T-scores. This calculation set the power of the test at 80% and the level of significance at 5%.

### Patients

The present study was part of a larger study<sup>22</sup> that aimed to investigate the changes in the jawbones by an advanced imaging technique (CBCT) among women with osteoporosis and those without, and the effect of osteoporosis medications on periodontal health. A secondary aim of this study was to investigate whether other structures that appear with jawbone scanning (e.g., cervical vertebrae) in dental CBCT images can be a better predictor of osteoporosis compared with the jawbones. The dental CBCT images taken by Barnkgkei et al.<sup>22</sup> for the previous investigation of 38 Syrian women (age range 47-75 years [mean = 57.9 (SD = 7.2)]) referred for a dual-energy X-ray absorptiometry examination by their physicians in Alassad Hospital—Damascus University in 2012, were analyzed in the present study.

Patients with diabetes, thyroid disorders, and bone diseases other than osteopenia or osteoporosis were excluded. None of the included women consumed alcohol; only 3 (7.9%) were smokers, and their smoking durations were 12, 18, and 40 years. None of participants had suffered a previous fracture in either the lumbar vertebrae or the femoral neck. Using the World Health Organization (WHO) criteria,<sup>23</sup> participants were classified according to their lumbar T-scores and femoral neck T-scores into 3 groups. Group A included women with healthy bone mineral density (BMD) values (T-score  $\geq -1$ ). Group B included women with osteopenia ( $-2.5 < \text{T-score} < -1$ ). Group C included women with osteoporosis (T-score  $\leq -2.5$ ). Ethical approval was obtained from the Damascus University Faculty of Dentistry Research Ethics Committee (no. 178/2011). In addition, informed consent was obtained from each participant.

### Radiographic devices and analysis software

The dual-energy X-ray absorptiometry examination was performed using a DXA scanner (Hologic Discovery QDR, Hologic Inc., Bedford 01730, MA). This device was calibrated daily in accordance with the manufacturer's recommendations. The lumbar spine (L1-L4) and the femoral neck were analyzed. T-scores were calculated from the young adult, normal, white reference databases as reported by the equipment manufacturer.

The CBCT images were taken using WhiteFox (de Gotzen S.r.l device, distributed by Satelec-Acteon Group Italy). The FOV and the voxel size were set at  $13 \times 15$  cm and 0.25 mm, respectively. The tube

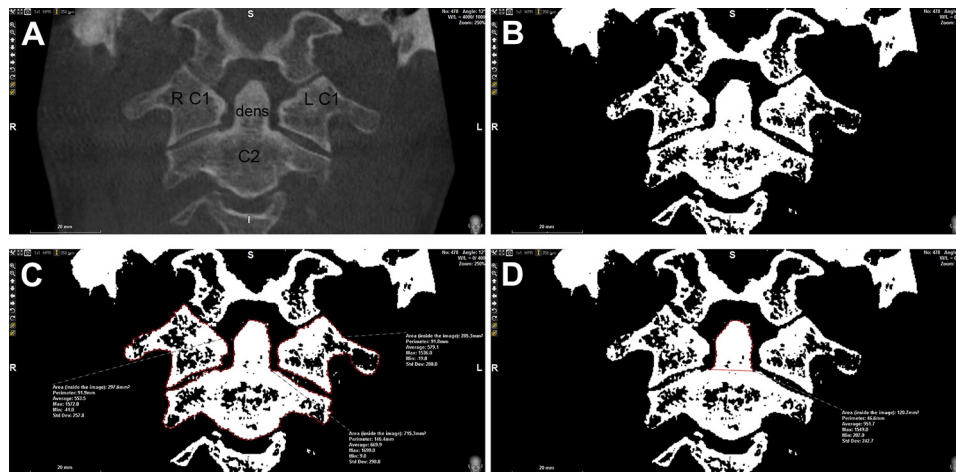


Fig. 1. **A**, The selected coronal slice after angulation adjustment of the cone beam computed tomography (CBCT) image. The right (R C1) and left (L C1) parts of the first and the second vertebrae (C2) with its odontoid process (dens) appear in this slide. **B**, Adjusting the window width and level to 0 and 400 gray values, respectively. **C**, Calculating the radiographic density (RD) of the left and right parts of the first and the second vertebrae. **D**, the dens.

current, tube voltage, and exposure time were preset at 9 mA, 105 kV, and 9 seconds; respectively. This device uses a pulsed mode acquisition. The effective dose from these parameters was about 100  $\mu$ SV (manufacturer’s information). The viewer software (WhiteFox Imaging, V3; developed by the same CBCT manufacturer) was used to analyze the CBCT images. This software is used by dentists to open and study CBCT scans because it contains basic tools (e.g., radiographic density calculator) and is also considered user-friendly. A personal laptop (Fujitsu, Lifebook AH 530) running Microsoft Windows 7 as an operating system was used to study and analyze the CBCT scans.

**Analysis of the CBCT scans**

The angulations of selected slices were adjusted manually to reduce the differences in head position among participants. This was done by navigating through the coronal slices at the mental foramen area to make the axial slices parallel to the plane that passes through the inferior border of both the right and left mental foramina.

The coronal slice that passes through the middle of the dens (the odontoid process of the second cervical vertebra) was selected in each CBCT scan. Both the first and second vertebrae in the selected slice were analyzed. In this slice, the first vertebra appears divided into 2 parts; right and left (Figure 1A).

To standardize the slice appearance among all studied cases and make the borders clearer, thereby reducing measurement variability (due to lack of sharpness of borders), the window width was adjusted

to zero. After changing the window width to zero, it was necessary to modify the window level because of the dominant trabecular bone composition of the vertebrae, making them nearly invisible in the default window level (1000 gray values). A window level of 400 gray values was subjectively chosen after attempts were made to find a suitable window level by using different window level values and comparing them with the default window width and level (4000 and 1000 gray values, respectively). This made the slices bicolor (white and black), where white indicated the bone tissue and black indicated all other tissues (Figure 1B).

To give an indication (although a limited one) of the variation in the measurement of RD between scans, the interscan RD homogeneity was tested by using distilled water, which was included during the scan of all participants. The mean RD of the distilled water (which was calculated in many areas of the resultant scans in the axial, coronal, and sagittal planes for all patients) was  $-225.7$  (SD = 55.1; range =  $-325$  to  $-123$ ) gray values. This standard deviation was comparable with that of the CBCT devices with low-noise tested in the study of Pauwels et al.<sup>24</sup> Moreover, considering the device’s bit depth (16 [i.e., 65,536 shades of gray]), the variation in the RD measurement of water (using the suggested calculation modality of Spin-Neto et al.<sup>25</sup>:  $[(-325 - (-123))/65536] \times 100$ ) was 0.31%. This indicated high homogeneity interscan densities and ensured the reliability of gray values in the present study. This finding was also demonstrated in a previous study.<sup>26</sup>

The CBCT-derived RD values were calculated for the first and second vertebrae and the dens using the

“measure polygon” tool with a magnification factor of 250%. The RD values of each side of the first vertebra were calculated separately (Figures 1C and 1D).

One examiner (IB), a PhD candidate in Oral Radiology with 5 years' experience, carried out the aforementioned analysis of CBCT scans. The analysis was repeated for a randomly selected subsample of 4 CBCT images (10% of the overall study sample) to establish intraexaminer agreement. A second examiner (LS; non-oral radiologist) repeated the measurements for the same subsample for the purpose of establishing the interexaminer agreement. Only the results of the main examiner (IB) were used in the present study analyses.

### Statistical analysis

Interclass correlation was carried out to assess intra-examiner and interexaminer agreement. Next, analysis of variance (ANOVA) tests and post hoc comparisons with Bonferroni correction were performed to investigate whether the differences in CBCT-derived RD values of the cervical vertebrae were statistically significant among the three study groups (healthy women, women with osteopenia, and women with osteoporosis). Thereafter, the Pearson correlation test was performed to estimate the strength of the correlation between cervical vertebrae RD values and lumbar vertebrae and femoral neck T-scores. The strength of correlation was considered weak, medium, and strong when correlation coefficient values were ( $0.2 < r \leq 0.4$ ), ( $0.4 < r < 0.7$ ) and ( $r \geq 0.7$ ), respectively.<sup>27</sup> Correlation coefficient values ranging between ( $0 < r \leq 0.2$ ) were regarded as showing no correlation. The diagnostic accuracy test (receiver operating characteristic analysis)<sup>28</sup> was performed to determine the validity of cervical vertebrae CBCT-derived RD gray values as a screening tool for femoral neck and lumbar vertebrae osteoporosis and decreased BMD. For this purpose, patients were regrouped into “osteoporotic” and “not osteoporotic” women as well as into “healthy” women and women with “decreased BMD (i.e., osteopenia or osteoporosis),” respectively. Based on receiver operating characteristic analyses, sensitivity, specificity, positive predictive values, negative predictive values, positive likelihood ratio, and negative likelihood ratio were calculated. Cutoff (threshold) values were determined in a way that enabled the highest sum of sensitivity and specificity.

In all statistical tests, the level of significance was set at 5%.

### RESULTS

The characteristics of the present study patients including age and body mass index in each group are summarized in Table I. Descriptive data of the cervical

**Table I.** Age and body mass index (BMI) of the study patients (n = 38)

Groups	Age (y), Mean (SD)	BMI, Mean (SD)
Groups according to the lumbar T-score		
Healthy (n = 10)	52.3 (3.5)	29.7 (5.3)
Osteopenia (n = 15)	59.1 (7.2)	31.7 (8.2)
Osteoporosis (n = 13)	60.9 (7.1)	28.5 (3.1)
Groups according to the femoral neck T-score		
Healthy (n = 17)	55.1 (4.6)	31 (7.5)
Osteopenia (n = 11)	58.1 (8.8)	30.4 (5.4)
Osteoporosis (n = 10)	62.6 (6.9)	28.4 (4.2)

vertebrae CBCT-derived RD values in each group are reported in Table II. Interclass correlation coefficients of the interexaminer and intraexaminer agreement for measuring the dens RD were 0.94 and 0.98, respectively, indicating excellent agreements. Coefficient values of the interexaminer and intraexaminer agreement were lower for the other areas (range 0.71-0.90), indicating good to excellent agreements.

There were statistically significant differences in the cervical vertebrae CBCT-derived RD values among the three groups (healthy women, women with osteopenia, and women with osteoporosis) whether classified according to lumbar vertebrae or femoral neck T-scores (Table II).

The strength of the correlation between the cervical vertebrae RD values and the T-scores of the lumbar vertebrae and the femoral neck are summarized in Table III. The dens CBCT-derived RD values showed the strongest correlation with lumbar vertebrae T-scores ( $r = 0.747$ ). Strong correlations were found between the first and second vertebrae RD values and the lumbar T-scores. Medium correlations were found between all cervical vertebrae RD values and the femoral neck T-scores ( $r = 0.5-0.6$ ).

Table IV summarizes the validity of cervical vertebrae CBCT-derived RD as a screening tool for osteoporosis. The sensitivity, specificity, and accuracy of all cervical vertebrae RD values, except those related to the left part of the first cervical vertebrae, were higher in predicting lumbar T-scores than in predicting femoral neck T-scores (see Table IV). Taking into account sensitivity, specificity, accuracy, and positive and negative likelihood ratios, the dens RD values were the best cervical vertebrae RD values in predicting lumbar vertebrae osteoporosis, whereas the CBCT-derived RD values of the left part of the first cervical vertebrae were the best cervical vertebrae RD values in predicting the femoral neck osteoporosis (Table IV). The cutoff gray values of the dens and the left part of the first cervical vertebrae CBCT-derived RD to predict osteoporosis were 600 and 391 for the lumbar

**Table II.** Description of the cervical vertebrae cone beam computed tomography (CBCT)-derived radiographic density (RD) values as gray values for healthy, osteopenic, and osteoporotic groups (mean [SD]) and the result of ANOVA test and post hoc comparisons with Bonferroni correction (n = 38)

Variable	According to lumbar T-score			According to femoral neck T-score		
	Healthy	Osteopenia	Osteoporosis	Healthy	Osteopenia	Osteoporosis
Right C1 vertebral GV	585 (90)	427 (58)*	361 (84)	503 (106)	445 (105)*	352 (87)
Left C1 vertebral GV	589 (127)	456 (59)*	376 (86)	533 (117)	446 (94)*	364 (74)
C2 vertebral GV	686 (69)	557 (92)†	438 (130)‡	619 (104)	532 (139)†	452 (135)
C2-Dens GV	882 (165)	701 (87)*	545 (109)§	787 (150)	692 (169)*	543 (115)

Numbers are rounded to whole numbers.

ANOVA test indicated statistical significant differences in all cervical vertebrae CBCT-derived RD values among the present study three groups. Only significant differences according to post hoc comparisons with Bonferroni correction were reported.

C, cervical; GV, gray value.

\*Significantly different from the healthy group ( $P < .005$ ).

†Significantly different from the healthy group ( $P < .05$ ).

‡Significantly different from the osteopenic group ( $P < .05$ ).

§Significantly different from the osteopenic group ( $P < .005$ ).

**Table III.** Pearson correlation coefficients (r) of the associations between the cervical vertebrae cone beam computed tomography (CBCT)-derived radiographic density (RD) values and the T-scores of the lumbar vertebrae and femoral neck (n = 38)

Variable	Lumbar vertebrae T-score	Femoral neck T-score
Right C1 vertebral GV	0.703 ( $P < .001$ )	0.516 ( $P = .001$ )
Left C1 vertebral GV	0.728 ( $P < .001$ )	0.590 ( $P < .001$ )
C2 vertebra GV	0.746 ( $P < .001$ )	0.504 ( $P = .001$ )
C2-Dens GV	0.747 ( $P < .001$ )	0.522 ( $P = .001$ )

C, cervical; GV, gray value.

vertebrae and the femoral neck, respectively. The positive and negative likelihood ratios indicated that the RD of the dens and the left part of the first cervical vertebrae ranged between being an “often useful” to a “sometimes useful” diagnostic test, thereby supporting their usefulness as a screening tool for osteoporosis.

The validity of cervical vertebrae CBCT-derived RD as a screening tool for decreased BMD (i.e., the presence of osteopenia or osteoporosis) is summarized in Table V. The sensitivity, specificity, and accuracy of all cervical vertebrae RD values, except those related to the left part of the first cervical vertebrae, were higher in predicting lumbar T-scores than in predicting femoral neck T-scores (Table V). Taking into account sensitivity, specificity, accuracy, and positive and negative likelihood ratios, the right part of the first cervical vertebrae CBCT-derived RD values were the best cervical vertebrae RD values in predicting lumbar vertebrae decreased mineral density, whereas the RD values of the left part of the first cervical vertebrae were the best cervical vertebrae RD values in predicting the femoral neck decreased mineral density (Table V). The cutoff gray values of the right and left parts of the first

cervical vertebrae RD to predict decreased BMD were 512 and 424 for the lumbar vertebrae and the femoral neck, respectively. The positive and negative likelihood ratios indicated that the RD of the right and left parts of the first cervical vertebrae ranged between being a “very useful” to a “sometimes useful” diagnostic test, thereby supporting their usefulness as a screening tool for decreased BMD.

## DISCUSSION

The present study suggests that cervical vertebrae CBCT-derived RD values can predict osteoporosis status in menopausal and postmenopausal women with use of the associated CBCT-viewer program. These findings could be considered as an important step in the collaboration between health care professionals to diagnose osteoporosis. Dentists can use CBCT images, exposed for appropriate diagnostic reasons, as an opportunistic screening tool for osteoporosis without the need for additional expensive and complicated programs or calibration phantoms. The CBCT viewer software, as a simple and available software used by dentists, offers the possibility of calculating the cervical vertebrae RD values that can indicate osteoporosis status. The present study findings suggest that the developer of the CBCT viewer software could add a new tool within its functions to automatically calculate the cervical vertebrae RD values and alert the dentist about referral when the possibility of osteoporosis is indicated.

The present study also shows that the correlations between the cervical vertebrae RD values and the lumbar T-scores were stronger than those between the cervical vertebrae RD values and the femoral neck T-scores. These findings are in keeping with the fact that the cervical and lumbar vertebrae are both trabecular in

**Table IV.** The validity of the cervical vertebrae cone beam computed tomography (CBCT)-derived radiographic density (RD) as a screening tool for femoral neck and lumbar vertebrae osteoporosis

Area	Variable	AUC (95% CI)	Cutoff value*	Sen	Spec	PPV	NPV	+LR	-LR
Lumbar vertebrae	Right C1 vertebral GV	0.845 (0.709-0.980)	383	76.9%	88%	76.9%	89.3%	7.18	0.26
	Left C1 vertebral GV	0.846 (0.712-0.980)	424	76.9%	84%	71.4%	87.5%	4.81	0.27
	C2 vertebral GV	0.865 (0.712-0.999)	475	84.6%	88%	78.6%	91.7%	7.05	0.17
	C2-Dens GV	0.908 (0.805-0.999)	600	76.9%	92%	83.3%	88.5%	9.6	0.25
Femoral Neck	Right C1 vertebral GV	0.832 (0.679-0.985)	383	80%	82.1%	61.5%	92%	4.48	0.24
	Left C1 vertebral GV	0.864 (0.737-0.991)	391	70%	92.9%	77.8%	89.7%	9.8	0.32
	C2 vertebral GV	0.779 (0.592-0.965)	560	90%	67.9%	50%	95%	2.8	0.15
	C2-Dens GV	0.857 (0.732-0.982)	698	100%	57.1%	45.5%	100%	2.33	0

AUC, area under the curve (accuracy); Sen, sensitivity; Spec, specificity; PPV, positive predictive value; NPV, negative predictive value; +LR, positive likelihood ratio; -LR, negative likelihood ratio.

\*In gray values. Rounded to whole numbers.

**Table V.** The validity of the cervical vertebrae cone beam computed tomography (CBCT)-derived radiographic density (RD) as a screening tool for femoral neck and lumbar vertebrae decreased mineral density

Area	Variable	AUC (95% CI)	Cutoff value*	Sen	Spec	PPV	NPV	+LR	-LR
Lumbar vertebrae	Right C1 vertebral GV	0.968 (0.917-0.999)	512	92.9%	90%	96.3%	81.8%	9.29	0.08
	Left C1 vertebral GV	0.893 (0.759-0.999)	534	92.9%	80%	92.9%	80%	4.64	0.09
	C2 vertebral GV	0.911 (0.815-0.999)	635	89.3%	90%	96.2%	75%	8.93	0.12
	C2-Dens GV	0.889 (0.771-0.999)	697	71.4%	90%	95.2%	52.9%	7.14	0.32
Femoral Neck	Right C1 vertebral GV	0.773 (0.622-0.924)	445	81%	70.6%	77.3%	75%	2.75	0.27
	Left C1 vertebral GV	0.812 (0.678-0.947)	424	61.9%	94.1%	92.9%	66.7%	10.52	0.4
	C2 vertebral GV	0.765 (0.611-0.918)	560	71.4%	82.4%	83.3%	70%	4.05	0.35
	C2-Dens GV	0.787 (0.641-0.934)	687	76.2%	76.5%	80%	72.2%	3.24	0.31

AUC, area under the curve (accuracy); Sen, sensitivity; Spec, specificity; PPV, positive predictive value; NPV, negative predictive value; +LR, positive likelihood ratio; -LR, negative likelihood ratio.

\*In gray values. Rounded to whole numbers.

nature and affected by menopause more than cortical bone.<sup>29</sup>

The present study findings could also be considered a first step toward distinguishing healthy women, women with osteopenia, and women with osteoporosis on the basis of cervical vertebrae CBCT-derived RD values. Thus, the present study demonstrated the possibility of identifying patients with osteopenia, going a step beyond previous research, which had aimed to develop a primary threshold to distinguish only between healthy women and those with osteoporosis.<sup>30</sup> Koh and Kim<sup>30</sup> used mandible CBCT-derived RD values in their study. The mandibular bone is affected to a lesser extent by osteoporosis compared with cervical vertebral bone. Thus, the cervical vertebrae RD values are more strongly correlated with the lumbar and femoral neck T-scores than are those of the mandible.<sup>22</sup> This might explain the possibility in the present study for distinguishing between women with osteopenia and those with osteoporosis when using the cervical vertebrae RD values. Needless to say, cervical vertebrae appear frequently in many dental radiographs and could be used for this purpose.

Among all cervical vertebrae CBCT-derived RD values, the RD values of the dens and the left part of the first cervical vertebrae were best in predicting the lumbar and femoral neck osteoporosis, respectively. In addition, based on the findings of the present study, the RD values of the dens and the left part of the first cervical vertebrae that are less than 600 and 391 gray values might suggest the presence of osteoporosis in the lumbar vertebrae and the femoral neck, respectively. With respect to predicting decreased BMD, the right and left parts of the first cervical vertebrae were best in predicting the lumbar and femoral neck decreased BMD (i.e., the presence of osteopenia or osteoporosis), respectively. The RD values of the right and left parts of the first cervical vertebrae that are less than 512 and 424 gray values might suggest the presence of osteopenia or osteoporosis in the lumbar vertebrae and the femoral neck, respectively.

One potential drawback of the present study is related to the limitation highlighted in the literature on the use of CBCT-derived gray values for RD measurement. CBCT-derived RD gray values are generally considered only to approximate bone density

values.<sup>27,31,32</sup> The inaccuracy of the RD calculation by CBCT arises from the increased scattering and noise levels, particularly at smaller voxel sizes; the cone-beam divergence phenomenon; the inferior detector efficiency; and the artifacts related to the scanner, which operates at a lower peak kilovoltage and a tube loading setting compared with MDCT. As a result, the signal-to-noise ratio in CBCT scanners is reduced compared with that in MDCT (the gold standard).<sup>33-38</sup>

Gray value inaccuracy was found to be worse in small FOVs.<sup>39-41</sup> In addition, variations exist between gray values from different CBCT devices and also between different parameters of the same CBCT device.<sup>42-44</sup> This is why the present study findings cannot be generalized to other CBCT devices or the same CBCT device with different exposure parameters. A recent review on CBCT<sup>45</sup> has recommended avoiding the use of CBCT gray values for bone quality assessment. However, the reliability of the CBCT gray values varies between the studies that have used them as an assessment tool for bone quality.<sup>46-48</sup> This, in turn, implies that the findings of each study should be critically reviewed and interpreted individually with regard to the acceptability of using CBCT gray values as a tool for bone quality assessment. Furthermore, the aforementioned systematic review<sup>45</sup> suggested using the bone structure analysis as an alternative tool to assess bone quality. The latter also depends on CBCT gray values because it is preceded by a threshold adjustment, a process that requires consistent RD measurements (reliable gray values) to obtain valid results. In other words, assuring the reliability of gray values is essential regardless of the analysis to be performed.

In the present study, the variation of RD measurement (interscan homogeneity) was tested (using distilled water), and the variation in gray values was 0.31%, which shows that the gray value calculation was highly homogeneous for all patients. However, this variation differs at different window levels. In other words, variation in gray values is not consistent across the Hounsfield unit (HU) spectrum. The latter implies that the interscan homogeneity score when scanning distilled water would not be identical to the score when scanning bone tissue. Thus, it is recommended that a reference material that has RD close to the RD of the region of interest be used.<sup>24,44</sup> The latter was not available in the present study. Yet, because vertebral bone is comprised mainly of trabecular bone, which has an RD of about 400 HU, using distilled water (HU = 0), although not being the best approach, might give some limited indication of the interscan homogeneity of the cervical vertebral RD.

A number of studies have found high correlations between the gray values of different CBCT scanners

both in vitro<sup>44,49</sup> and in vivo,<sup>50</sup> and between CBCT gray values and MDCT HU values.<sup>48,51,52</sup> Nevertheless, these correlations and regression equations (to convert gray values to equivalent HU) are restricted to the evaluated CBCT devices and the test conditions and cannot be extrapolated or generalized to other devices.<sup>45</sup>

Further, confirmatory studies with larger sample sizes are needed to confirm the findings of the present study regarding the validity of the cervical vertebrae CBCT-derived RD values as a tool in predicting the osteoporosis status in menopausal and postmenopausal women.

## CONCLUSIONS

When CBCT scans are obtained for appropriate dental indications, dentists can play an important role in the opportunistic screening of osteoporosis and referring suspicious cases to specialists' care. Cervical vertebrae appear frequently in many dental radiographs. Their CBCT-derived RD values can predict BMD status in menopausal and postmenopausal women by using the associated viewer program of the CBCT. The RD values of the dens and the left part of the first cervical vertebrae showed the strongest correlation with T-scores and the highest sensitivity, specificity, and accuracy in predicting osteoporosis in lumbar vertebrae and the femoral neck, respectively. The cutoff gray values of the dens and the left part of the first cervical vertebrae CBCT-derived RD to predict osteoporosis were 600 and 391 for the lumbar vertebrae and the femoral neck, respectively. Also, the right and left parts of the first cervical vertebrae showed the highest sensitivity, specificity, and accuracy in predicting decreased BMD in the lumbar vertebrae and the femoral neck, respectively. The cutoff values were 512 GV and 424 GV, respectively. The present study's findings should be confirmed on other CBCT devices.

## REFERENCES

1. National Institutes of Health Consensus Development Panel on Osteoporosis Prevention Diagnosis and Therapy. Osteoporosis prevention, diagnosis, and therapy. *JAMA*. 2001;285:785-795.
2. Stone KL, Seeley DG, Lui LY, et al. BMD at multiple sites and risk of fracture of multiple types: long-term results from the Study of Osteoporotic Fractures. *J Bone Miner Res*. 2003;18:1947-1954.
3. Kasturi GC, Cifu DX, Adler RA. A review of osteoporosis: Part I. Impact, pathophysiology, diagnosis and unique role of the physiatrist. *PMR*. 2009;1:254-260.
4. Genant HK, Engelke K, Prevrhal S. Advanced CT bone imaging in osteoporosis. *Rheumatology (Oxford)*. 2008;47:iv9-iv16.
5. Cummings SR, Melton LJ. Epidemiology and outcomes of osteoporotic fractures. *Lancet*. 2002;359:1761-1767.
6. Kado DM, Browner WS, Palermo L, Nevitt MC, Genant HK, Cummings SR. Vertebral fractures and mortality in older women: a prospective study. Study of Osteoporotic Fractures Research Group. *Arch Intern Med*. 1999;159:1215-1220.

7. Becker DJ, Kilgore ML, Morrisey MA. The societal burden of osteoporosis. *Curr Rheumatol Rep*. 2010;12:186-191.
8. Guglielmi G. Preface. Imaging of osteoporosis. *Radiol Clin North Am*. 2010;48:xv.
9. Giro G, Chambrone L, Goldstein A, et al. Impact of osteoporosis in dental implants: a systematic review. *World J Orthop*. 2015;6:311-315.
10. Nackaerts O, Jacobs R, Devlin H, et al. Osteoporosis detection using intraoral densitometry. *Dentomaxillofac Radiol*. 2008;37:282-287.
11. Verheij JG, Geraets WG, van der Stelt PF, et al. Prediction of osteoporosis with dental radiographs and age. *Dentomaxillofac Radiol*. 2009;38:431-437.
12. Geraets WG, Verheij JG, van der Stelt PF, et al. Osteoporosis and the general dental practitioner: Reliability of some digital dental radiological measures. *Community Dent Oral Epidemiol*. 2007;35:465-471.
13. Fyhrie DP. Summary—measuring “bone quality.”. *J Musculoskeletal Neuronal Interact*. 2005;5:318-320.
14. Muller R. Bone microarchitecture assessment: current and future trends. *Osteoporos Int*. 2003;14:S89-S95:discussion S99.
15. White SC, Pharoah MJ. The evolution and application of dental maxillofacial imaging modalities. *Dent Clin North Am*. 2008;52:689-705.
16. Mozzo P, Procacci C, Tacconi A, Martini PT, Andreis IA. A new volumetric CT machine for dental imaging based on the cone-beam technique: Preliminary results. *Eur Radiol*. 1998;8:1558-1564.
17. Bornstein MM, Scarfe WC, Vaughn VM, Jacobs R. Cone beam computed tomography in implant dentistry: a systematic review focusing on guidelines, indications, and radiation dose risks. *Int J Oral Maxillofac Implants*. 2014;29:55-77.
18. Pauwels R, Beinsberger J, Collaert B, et al. Effective dose range for dental cone beam computed tomography scanners. *Eur J Radiol*. 2012;81:267-271.
19. Li G. Patient radiation dose and protection from cone-beam computed tomography. *Imaging Sci Dent*. 2013;43:63-69.
20. SedentextCT Project Radiation Protection. Cone Beam CT for Dental and Maxillofacial Radiology. *Provisional guidelines*; 2009. Available at: [http://www.sedentext.eu/system/files/sedentext\\_project\\_provisional\\_guidelines.pdf](http://www.sedentext.eu/system/files/sedentext_project_provisional_guidelines.pdf). Accessed September 8, 2015.
21. Hua Y, Nackaerts O, Duyck J, Maes F, Jacobs R. Bone quality assessment based on cone beam computed tomography imaging. *Clin Oral Implants Res*. 2009;20:767-771.
22. Barnkgei I, Al Haffar I, Khattab R. Osteoporosis prediction from the mandible using cone-beam computed tomography. *Imaging Sci Dent*. 2014;44:263-271.
23. World Health Organization. Assessment of fracture risk and its application to screening for postmenopausal osteoporosis. Report of a WHO Study Group. *World Health Organ Tech Rep Ser*. 1994;843:1-129.
24. Pauwels R, Stamatakis H, Manousaridis G, et al. Development and applicability of a quality control phantom for dental cone-beam CT. *J Appl Clin Med Phys*. 2011;12:3478.
25. Spin-Neto R, Gotfredsen E, Wenzel A. Standardized method to quantify the variation in voxel value distribution in patient-simulated CBCT data sets. *Dentomaxillofac Radiol*. 2015;44:20140283.
26. Sennerby L, Andersson P, Pagliani L, et al. Evaluation of a novel cone beam computed tomography scanner for bone density examinations in preoperative 3D reconstructions and correlation with primary implant stability [e-pub ahead of print]. *Clin Implant Dent Relat Res*; 2013. Epub ahead of print; <http://dx.doi.org/10.1111/cid.12193>. Accessed September 8, 2015.
27. Naitoh M, Kurosu Y, Inagaki K, Katsumata A, Noguchi T, Ariji E. Assessment of mandibular buccal and lingual cortical bones in postmenopausal women. *Oral Surg Oral Med Oral Pathol Oral Radiol Endod*. 2007;104:545-550.
28. Florkowski CM. Sensitivity, specificity, receiver-operating characteristic (ROC) curves and likelihood ratios: communicating the performance of diagnostic tests. *Clin Biochem Rev*. 2008;29:S83-S87.
29. Osteoporosis. Part I. Advanced radiologic assessment using quantitative computed tomography. *West J Med*. 1983;139:75-84.
30. Koh KJ, Kim KA. Utility of the computed tomography indices on cone beam computed tomography images in the diagnosis of osteoporosis in women. *Imaging Sci Dent*. 2011;41:101-106.
31. Naitoh M, Katsumata A, Mitsuya S, Kamemoto H, Ariji E. Measurement of mandibles with microfocus x-ray computerized tomography and compact computerized tomography for dental use. *Int J Oral Maxillofac Implants*. 2004;19:239-246.
32. Casseta M, Stefanelli LV, Di Carlo S, Pompa G, Barbato E. The accuracy of CBCT in measuring jaws bone density. *Eur Rev Med Pharmacol Sci*. 2012;16:1425-1429.
33. Schulze R, Heil U, Gross D, et al. Artefacts in CBCT: a review. *Dentomaxillofac Radiol*. 2011;40:265-273.
34. Rinkel J, Gerfault L, Esteve F, Dinten JM. A new method for x-ray scatter correction: first assessment on a cone-beam CT experimental setup. *Phys Med Biol*. 2007;52:4633-4652.
35. Quereshy FA, Savell TA, Palomo JM. Applications of cone beam computed tomography in the practice of oral and maxillofacial surgery. *J Oral Maxillofac Surg*. 2008;66:791-796.
36. Hassan B, Couto Souza P, Jacobs R, de Azambuja Berti S, van der Stelt P. Influence of scanning and reconstruction parameters on quality of three-dimensional surface models of the dental arches from cone beam computed tomography. *Clin Oral Investig*. 2010;14:303-310.
37. Gupta R, Grasruck M, Suess C, et al. Ultra-high resolution flat-panel volume CT: fundamental principles, design architecture, and system characterization. *Eur Radiol*. 2006;16:1191-1205.
38. Orth RC, Wallace MJ, Kuo MD; Technology Assessment Committee of the Society of Interventional Radiology. C-arm cone-beam CT: general principles and technical considerations for use in interventional radiology. *J Vasc Interv Radiol*. 2008;19:814-820.
39. Katsumata A, Hirukawa A, Okumura S, et al. Effects of image artifacts on gray-value density in limited-volume cone-beam computerized tomography. *Oral Surg Oral Med Oral Pathol Oral Radiol Endod*. 2007;104:829-836.
40. Katsumata A, Hirukawa A, Okumura S, et al. Relationship between density variability and imaging volume size in cone-beam computerized tomographic scanning of the maxillofacial region: an in vitro study. *Oral Surg Oral Med Oral Pathol Oral Radiol Endod*. 2009;107:420-425.
41. Molteni R. Prospects and challenges of rendering tissue density in Hounsfield units for cone beam computed tomography. *Oral Surg Oral Med Oral Pathol Oral Radiol*. 2013;116:105-119.
42. Chindasombatjaroen J, Kakimoto N, Shimamoto H, Murakami S, Furukawa S. Correlation between pixel values in a cone-beam computed tomographic scanner and the computed tomographic values in a multidetector row computed tomographic scanner. *J Comput Assist Tomogr*. 2011;35:662-665.
43. Parsa A, Ibrahim N, Hassan B, Motroni A, van der Stelt P, Wismeijer D. Influence of cone beam CT scanning parameters on grey value measurements at an implant site. *Dentomaxillofac Radiol*. 2013;42:79884780.
44. Pauwels R, Nackaerts O, Bellaiche N, et al. Variability of dental cone beam CT grey values for density estimations. *Br J Radiol*. 2013;86:20120135.

45. Pauwels R, Jacobs R, Singer SR, Mupparapu M. CBCT-based bone quality assessment: are Hounsfield units applicable? *Dentomaxillofac Radiol*. 2015;44:20140238.
46. Hao Y, Zhao W, Wang Y, Yu J, Zou D. Assessments of jaw bone density at implant sites using 3D cone-beam computed tomography. *Eur Rev Med Pharmacol Sci*. 2014;18:1398-1403.
47. Nemtoi A, Ladunca O, Dragan E, Budacu C, Mihai C, Haba D. Quantitative and qualitative bone assessment of the posterior mandible in patients with diabetes mellitus: a cone beam computed tomography study. *Rev Med Chir Soc Med Nat Iasi*. 2013;117:1002-1008.
48. Parsa A, Ibrahim N, Hassan B, van der Stelt P, Wismeijer D. Bone quality evaluation at dental implant site using multislice CT, micro-CT, and cone beam CT. *Clin Oral Implants Res*. 2015;26:e1-e7.
49. Mah P, Reeves TE, McDavid WD. Deriving Hounsfield units using grey levels in cone beam computed tomography. *Dentomaxillofac Radiol*. 2010;39:323-335.
50. Reeves TE, Mah P, McDavid WD. Deriving Hounsfield units using grey levels in cone beam CT: a clinical application. *Dentomaxillofac Radiol*. 2012;41:500-508.
51. Parsa A, Ibrahim N, Hassan B, Motroni A, van der Stelt P, Wismeijer D. Reliability of voxel gray values in cone beam computed tomography for preoperative implant planning assessment. *Int J Oral Maxillofac Implants*. 2012;27:1438-1442.
52. Nomura Y, Watanabe H, Honda E, Kurabayashi T. Reliability of voxel values from cone-beam computed tomography for dental use in evaluating bone mineral density. *Clin Oral Implants Res*. 2010;21:558-562.

*Reprint requests:*

Imad Barnkgkei, BDS, MSc  
Oral Medicine Department  
Faculty of Dentistry  
Damascus University  
Mazzeah Highway  
Damascus  
Syria  
Imadbarn@gmail.com